
Formation of novel rare-gas-containing molecules by molecular photodissociation in clusters

Arie Cohen,^a Masha Y. Niv^a and R. Benny Gerber^{*ab}

^a Department of Physical Chemistry and The Fritz Haber Research Center, The Hebrew University, Jerusalem 91904, Israel. E-mail: benny@fh.huji.ac.il

^b Department of Chemistry, University of California, Irvine, CA 92697, USA

Received 14th December 2000

First published as an Advance Article on the web 4th June 2001

Recent work by Räsänen and coworkers showed that photolysis of hydrides in rare-gas matrices results in part in formation of novel, rare-gas-containing molecules. Thus, photolysis of HCl in Xe and of H₂O in Xe result respectively in formation of HXeCl and HXeOH in the Xe matrices. *Ab initio* calculations show that the compounds HRgY so formed are stable in isolation, and that by the strength and nature of the bonding these are molecules, very different from the corresponding weakly bound clusters Rg_n··HY. This paper presents a study of the formation mechanism of HRgY following the photolysis of HY in clusters Rg_n(HY). Calculations are described for HXeCl, as a representative example. Potential energy surfaces that govern the formation of HXeCl in the photolysis of HCl in xenon clusters are obtained, and the dynamics on these surfaces is analyzed, partly with insight from trajectories of molecular dynamics simulations. The potential surfaces are obtained by a new variant of the DIM (diatomics in molecules) and DIIS (diatomics in ionic systems) models. Non-adiabatic couplings are also obtained. The main results are: (1) Properties of HXeCl predicted by the DIM–DIIS model are in reasonable accord with results of *ab initio* calculations. (2) The potential along the isomerization path HXeCl → Xe··HCl predicted by DIM is in semiquantitative accord with the *ab initio* results. (3) Surface-hopping molecular dynamics simulations of the process in clusters, with “on the fly” calculations of the DIM–DIIS potentials and non-adiabatic couplings are computationally feasible. (4) Formation of HXeCl, following photolysis of HCl in Xe_{5,4}(HCl), requires cage-exit of the H atom as a precondition. The H atom and the Cl can then attack the same Xe atom on opposite sides, leading to charge transfer and production of the ionic HXeCl. (5) Non-adiabatic processes play an important role, both in the reagent configurations, and at the charge-transfer stage. The results open the way to predictions of the formation of new HRgY species.

I. Introduction

The chemical inertness of the rare-gas atoms in their electronic ground state was widely accepted as a dogma in the molecular sciences for many years. Exceptions were recognized when Bartlett and his coworkers were able to prepare the first xenon-containing compound, Xe[PtF₆] in 1962.¹ In the years that followed several other molecules that contain xenon, radon or krypton were

obtained.^{2–4} The domain of rare-gas chemistry so initiated remained, however, limited to a relatively narrow class of compounds. The fact that the rare gases are chemically inert with regard to most molecular and atomic species is used in areas such as matrix-isolation spectroscopy: in this field free radicals and other very reactive species are trapped in rare-gas matrices, in which they are stable and their properties can be conveniently studied. Rare-gas solids and clusters have also been extensively used as media for exploring fundamental chemical reactions in condensed phases.⁵ There are obvious advantages of simplicity of interpretation in studying *e.g.* cage effects and other environmental effects on a reaction in a medium that is itself chemically inert. Indeed, the study of photodissociation and recombination of small molecules such as HCl, H₂O, I₂, *etc.* in rare-gas solids and clusters has emerged in itself as an important and active subject in the framework of condensed-phase photochemistry.^{5–16}

A surprising and important development in the field came, however, from recent work by Räsänen and his group in Helsinki. They found that photolysis of certain hydrides HX (*e.g.* HCl, H₂O, HCNO *etc.*) in rare-gas matrices results (in addition to photodissociation and recombination) in the production of a new class of rare-gas-containing molecules, HRgX.^{16–21} The first studies were done in solid xenon, and led to the identification of molecules such as HXeCl, HXeI, HXeOH, HXeNCO, *etc.* Krypton-containing compounds were likewise prepared, and in an exciting development, the Räsänen group was able to confirm the production of HArF, the first argon-containing stable molecule, upon photolysis of HF in a matrix.²¹ These results are intriguing because a new and potentially-rich class of rare-gas-containing molecules is introduced, with properties that seem very interesting.

There is, however, another question of importance to explore—what are the formation mechanisms of the new molecules. Given the weak binding forces between Rg and a hydride HX in the ground electronic state, it is interesting to determine the interaction potential and the dynamics in time that leads to the formation of HRgX, *e.g.* HXeCl, where the rare-gas atom is chemically bound, both in terms of the strength of the bond and nature of the interactions. The present study explores this question. Potential energy surfaces (PESs) that describe the formation of HXeCl, following photolysis of HCl in xenon clusters, are constructed. The reaction pathways on these potentials are examined qualitatively, and some dynamics simulations are carried out. Insight into the mechanism of the reaction is obtained.

In previous studies, the electronic structure of several HRgX molecules was computed by *ab initio* methods,^{16,18,22–24} and also the vibrational spectroscopy of these molecules was obtained from *ab initio* PES points.^{22–24} The success of the spectroscopy calculations establishes the validity of these potential energy points from the *ab initio* calculations. However, these are confined to a small vicinity of the equilibrium configuration. For our purpose, global PESs are required, and of a type that can be used in molecular dynamics (MD) simulations. The semiempirical potentials provided here are suitable for this purpose. In the following section we discuss the construction of the PESs, and briefly comment on the MD simulation method. In Section III, results are presented and discussed. Concluding remarks are presented in Section IV.

II. Model and methods

II.a. Extended DIM–DIIS potential surfaces for HRgX

To study the dynamics leading to formation of HRgX a global potential is required that describes the Rg + HX reagent, the product species and the intermediate configurations that may be involved. It is further important to have an analytical potential, or one that can be computed efficiently on the fly, along trajectories that describe the dynamics. DIM^{25–27} type potentials meet these requirements. Our choice of a potential of this type is motivated in part by the fact that DIM interactions were employed by our group in extensive simulations of photodissociation and recombination of HCl in solid Ar,¹² and in argon clusters.^{16,28,29} Evidence for the success of DIM in these applications is encouraging at least with respect to the description of the reagent configurations in the process considered here. DIM potentials proved successful in the hands of several other authors in studies of other photodissociation and recombination processes in rare-gas solids.^{5,10}

Consider first the DIM as applied to the $\text{Xe}_n(\text{HCl})$, in a framework where the photodissociation and recombination channels only are considered. Following closely the model of ref. 12 and 16, the $\text{H}(\text{S}) + \text{Cl}({}^2\text{P})$ interaction is described in a valence-bond type of framework, using two effective electrons, with an S-orbital located on the hydrogen atom, and p-type orbitals on the Cl, which asymptotically is produced in a ${}^2\text{P}$ state upon dissociation. The two possible spin states of each of the electrons, and the three possible p-type orbitals for the effective (unpaired) p-type electron on the Cl, result in a total of 12 states, including both singlets and triplets.^{12,16} The interaction of a rare-gas atom with $\text{H}(\text{S}) + \text{Cl}({}^2\text{P})$ is modeled as follows: An isotropic potential of the Lennard-Jones form or similar is used for $\text{H}(\text{S}) + \text{Rg}$. Such potentials are available from scattering or other gas-phase data, or from *ab initio* calculations.^{12,13,16} For $\text{Cl}({}^2\text{P}) + \text{Rg}$, the interaction is assumed to be of the form:¹⁶

$$V(r, \gamma) = V_0(r) + V_2(r)P_2(\cos \gamma) \quad (1)$$

where r is the distance between Rg and Cl and γ can be viewed as the orientation angle between the p-orbital on the $\text{Cl}({}^2\text{P})$, and the distance vector r between the two atoms. The angle γ is thus an electronic coordinate. To obtain the adiabatic PESs of $[\text{H}(\text{S}) + \text{Cl}({}^2\text{P})]/\text{Rg}$, the interaction potential (1) is represented in the basis p_x, p_y, p_z of the effective electron of chlorine. Then the spin-orbit coupling operator $\xi\mathbf{L}\cdot\mathbf{S}$ is added to this interaction (\mathbf{L} is the electronic angular momentum, and \mathbf{S} is the total spin). It is assumed that ξ , the spin-orbit coupling parameter, is due to the Cl atom only. The matrix $V + \xi\mathbf{L}\cdot\mathbf{S}$ in the p-orbital representation is then diagonalized. Extension of the calculation for systems with more rare-gas atoms is straightforward, using pairwise Rg-Rg potentials for the interaction between the rare-gas atoms themselves.^{12,16}

The above approach, along the original lines of DIM^{25,26} does not contain any mechanism for the formation of a chemically-bound species HRgX. Indeed, *ab initio* calculations by Johansson *et al.*³⁰ and by Lundell *et al.*²³ show that HXeCl is bound partly by covalent and partly by ionic interactions. At equilibrium configuration, the system has a strongly ionic character described approximately by the atomic point charges: $\text{H}(-0.157) \text{Xe}(+0.777) \text{Cl}(-0.620)$, a situation that cannot be described by DIM.

To extend the model and allow for the description of HRgX, we use a variant of the DIIS approach, due to Last and George.^{31,32} In essence, the model employed describes the wavefunction of the system as a linear combination of three virtual "species": $[\text{H}(\text{S}) + \text{Cl}({}^2\text{P})]/\text{Rg}$, as described by DIM above, and the ionic species $[\text{H}(\text{S}) + \text{Xe}^+(\text{P})]/\text{Cl}^-$, $\text{H}^-/[\text{Xe}^+(\text{P}) + \text{Cl}(\text{P})]$. The original treatment of Last and George of HXeCl includes only the ionic species $[\text{H}(\text{S}) + \text{Xe}^+(\text{P})]/\text{Cl}^-$: The incorporation of the second ionic species is straightforward and quantitatively crucial.

As in the neutral DIM "species", each of the ionic species is treated by a two effective electrons model. The interaction between $\text{H}(\text{S})$ and $\text{Xe}^+(\text{P})$ is modeled in a valence-bond framework, with an S-orbital on the H, and a p-orbital basis on $\text{Xe}^+(\text{P})$, the latter described by a single effective electron. An isotropic atom-atom interaction is used for $\text{H}(\text{S})/\text{Cl}^-$, while an anisotropic interaction, of the form of eqn. (1), is required for $\text{Xe}^+(\text{P})/\text{Cl}^-$. All the necessary input is obtainable from *ab initio* calculations or from empirical data for diatoms only: $\text{H}(\text{S})/\text{Cl}^-$, $\text{Xe}^+(\text{P})/\text{Cl}^-$ and $\text{H}/\text{Xe}^+(\text{P})$. The number of basis states restricted to this ionic species is 12. The spin-orbit coupling effect is predominantly due to $\text{Xe}^+(\text{P})$, and can be included as described above for the neutral species. The two-electron model for the species $\text{H}^-/[\text{Xe}^+(\text{P}) + \text{Cl}(\text{P})]$ uses a valence-bond description of the interaction between $\text{Xe}^+(\text{P})$ and $\text{Cl}(\text{P})$, with one effective electron in a p-type orbital on $\text{Xe}^+(\text{P})$ and an effective electron in a p-type orbital on the $\text{Cl}(\text{P})$. The total number of states of this ionic species is thus 36. Again, all the input information for this species was obtained from *ab initio* calculations on diatomic systems ($\text{H}^-/\text{Xe}^+(\text{P})$; $\text{H}^-/\text{Cl}(\text{P})$) only, or from empirical data for the diatomics. For example, the interaction energies for $\text{H}^-/\text{Xe}^+(\text{P})$ were extracted from excited state *ab initio* calculations for HXe .

To complete the construction of the DIM-DIIS model for the Hamiltonian of the system, couplings between states of each two of the different species must be provided:

$$\begin{aligned} H_{\text{N},11} &\equiv \langle \Psi_{\text{N}} | H | \Psi_{12} \rangle \\ H_{\text{N},12} &\equiv \langle \Psi_{\text{N}} | H | \Psi_{12} \rangle \\ H_{11,12} &\equiv \langle \Psi_{11} | H | \Psi_{12} \rangle \end{aligned} \quad (2)$$

where H is the electronic Hamiltonian of the system, and the labels N, I1, I2 refer respectively to the neutral and to the two ionic species:

$$\begin{aligned}\Psi_N &= \Psi(\text{Xe} \cdots \text{HCl}) \\ \Psi_{I1} &= \Psi(\text{Xe}^+ \text{H}^- \text{Cl}) \\ \Psi_{I2} &= \Psi(\text{Xe}^+ \text{HCl}^-)\end{aligned}\quad (3)$$

(The order of the atoms in this notation is, of course, just arbitrary.)

Within the two effective electrons DIM–DIIS model used here, the coupling $H_{N,I1}$ between the neutral species and $\text{Xe}^+ \text{H}^- \text{Cl}$ is associated with the electron transfer process $\text{HXeH}^- \text{Xe}^+$. It can be extracted from *ab initio* calculations on the coupling between neutral and ionic states in this diatomic system. Likewise, $H_{N,I2}$ can be extracted from the coupling between ionic and neutral states in $\text{XeClXe}^+ \text{Cl}^-$ as was indeed done by Last and George.³² $H_{I1,I2}$ was determined from *ab initio* calculations on the species $(\text{HCl})^-$, by considering the relative contributions of states with excess electron localized on the chlorine, and states where it is localized on the hydrogen. The electron is, however, predominantly localized on the Cl, to an extent that $H_{I1,I2}$ is small.

The structure of the Hamiltonian matrix in the DIM–DIIS model used here for the system $\text{H} + \text{Xe} + \text{Cl}$ is shown in Table 1. This Table is given only for *linear* configurations of the triatomic system. In Table 1, S are single states, T_{-1} , T_0 and T_1 are triplet states (corresponding to $\beta\beta$, $2\beta + \alpha\beta$, $\alpha\alpha$, spin configurations of the two effective electrons). In Table 1, A is a third of the spin–orbit splitting of $\text{Cl}(^2\text{P})$, C is a third of the spin–orbit splitting of $\text{Xe}(^1\text{P})$. The roles of the potential terms V_j and the coupling elements U_n listed in Table 1 are defined in Table 2, where the

Table 1 Structure of the Hamiltonian matrix of $\text{H} + \text{Xe} + \text{Cl}$. The matrix shown is for collinear configurations only, in a DIM–DIIS basis of 26 states. Both neutral and ion-pair states are included. S corresponds to singlets, T_{-1} , T_0 , T_1 correspond to triplet states

HCIXe				H ⁺ Xe ⁺ Cl	HXe ⁺ Cl ⁻			
S	T ₋₁	T ₀	T ₁	¹ Σ ³ Π	S	T ₋₁	T ₀	T ₁
V_1 0 0 0 V_2 0 0 0 V_1	0 0 0 A 0 0 0 A 0	A 0 0 0 0 0 0 0 -A	0 -A 0 0 0 -A 0 0 0	0 0 U_5 0 0 0	U_1 0 0 0 U_2 0 0 0 U_1	0 0 0 0 0 0 0 0 0	0 0 0 0 0 0 0 0 0	0 0 0 0 0 0 0 0 0
0 A 0 0 0 A 0 0 0	$V_3 - A$ 0 0 0 V_4 0 0 0 $V_3 + A$	0 A 0 0 0 A 0 0 0	0 0 0 0 0 0 0 0 0	0 U_6 0 0 0 U_6	0 0 0 0 0 0 0 0 0	U_3 0 0 0 U_4 0 0 0 U_3	0 0 0 0 0 0 0 0 0	0 0 0 0 0 0 0 0 0
A 0 0 0 0 0 0 0 -A	0 0 0 A 0 0 0 A 0	V_3 0 0 0 V_4 0 0 0 V_3	0 A 0 0 0 A 0 0 0	0 U_6 0 0 0 U_6	0 0 0 0 0 0 0 0 0	0 0 0 0 0 0 0 0 0	U_3 0 0 0 U_4 0 0 0 U_3	0 0 0 0 0 0 0 0 0
0 0 0 -A 0 0 0 -A 0	0 0 0 0 0 0 0 0 0	0 0 0 A 0 0 0 A 0	$V_3 + A$ 0 0 0 V_4 0 0 0 $V_3 - A$	0 U_6 0 0 0 U_6	0 0 0 0 0 0 0 0 0	0 0 0 0 0 0 0 0 0	0 0 0 0 0 0 0 0 0	U_3 0 0 0 U_4 0 0 0 U_3
0 U_5 0 0 0 0	0 0 0 U_6 0 U_6	0 0 0 U_6 0 U_6	0 0 0 U_6 0 U_6	$V_5 - \sqrt{2}C$ $-\sqrt{2} C V_6$	0 U_7 0 0 0 0	0 0 0 U_8 0 U_8	0 0 0 U_8 0 U_8	0 0 0 U_8 0 U_8
U_1 0 0 0 U_2 0 0 0 U_1	0 0 0 0 0 0 0 0 0	0 0 0 0 0 0 0 0 0	0 0 0 0 0 0 0 0 0	0 0 U_7 0 0 0	V_7 0 0 0 V_8 0 0 0 V_7	0 0 0 C 0 0 0 C 0	C 0 0 0 0 0 0 0 -C	0 -C 0 0 0 -C 0 0 0
0 0 0 0 0 0 0 0 0	U_3 0 0 0 U_4 0 0 0 U_3	0 0 0 0 0 0 0 0 0	0 0 0 0 0 0 0 0 0	0 U_8 0 0 0 U_8	0 C 0 0 0 C 0 0 0	$V_9 - C$ 0 0 0 V_{10} 0 0 0 $V_9 + C$	0 C 0 0 0 C 0 0 0	0 0 0 0 0 0 0 0 0
0 0 0 0 0 0 0 0 0	0 0 0 0 0 0 0 0 0	U_3 0 0 0 U_4 0 0 0 U_3	0 0 0 0 0 0 0 0 0	0 U_8 0 0 0 U_8	C 0 0 0 0 0 0 0 -C	0 0 0 C 0 0 0 C 0	V_9 0 0 0 V_{10} 0 0 0 V_9	0 C 0 0 0 C 0 0 0
0 0 0 0 0 0 0 0 0	0 0 0 0 0 0 0 0 0	0 0 0 0 0 0 0 0 0	U_3 0 0 0 U_4 0 0 0 U_3	0 U_8 0 0 0 U_8	0 0 0 -C 0 0 0 -C 0	0 0 0 0 0 0 0 0 0	0 0 0 C 0 0 0 C 0	$V_9 + C$ 0 0 0 V_{10} 0 0 0 $V_9 - C$

Table 2 Interaction and coupling terms in the DIM–DIIS Hamiltonian for H + X + Cl

Interaction parameter ^a	Role	Source
V_1, V_2	$^1\Pi, ^1\Sigma$	Ref. 33
V_3, V_4	$^3\Pi$ and $^3\Sigma$ of HCl	
V_5	$^1\Sigma$ of Xe^+Cl	
V_6	$^3\Pi$ of Xe^+Cl	<i>Ab initio</i>
V_7, V_8	$^1\Pi, ^1\Sigma$	Ref. 34
V_9, V_{10}	$^3\Pi$ and $^3\Sigma$ of HXe^+	
	ion/neutral coupling for:	
U_1	$^1\Pi \text{XeCl} \leftrightarrow ^1\Pi \text{Xe}^+\text{Cl}^-$	
U_2	$^1\Sigma \text{XeCl} \leftrightarrow ^1\Sigma \text{Xe}^+\text{Cl}^-$	Ref. 31
U_3	$^3\Pi \text{XeCl} \leftrightarrow ^3\Pi \text{Xe}^+\text{Cl}^-$	
U_4	$^3\Sigma \text{XeCl} \leftrightarrow ^3\Sigma \text{Xe}^+\text{Cl}^-$	
U_5	$^1\Sigma \text{HCl} \leftrightarrow ^1\Sigma \text{Xe}^+\text{Cl}$	<i>Ab initio</i>
U_6	$^3\Pi \text{HCl} \leftrightarrow ^3\Pi \text{Xe}^+\text{Cl}$	<i>Ab initio</i>
U_7	$^1\Sigma \text{HXe}^+ \leftrightarrow ^1\Sigma \text{Xe}^+\text{Cl}$	<i>Ab initio</i>
U_8	$^3\Pi \text{HXe}^+ \leftrightarrow ^3\Pi \text{Xe}^+\text{Cl}$	<i>Ab initio</i>

^a The interactions V_j are within a given neutral or ionic species. Coupling elements U_n are between species.

sources from which they were determined are listed. The Hamiltonian matrix for DIM–DIIS in Table 1 is given for a basis set of 26 states, which is only a subset of the full manifold of the 60 relevant states. The matrix shows both the Hamiltonian elements pertinent to the species N, I1, I2, and to the couplings between the species. As was found in the calculations, formation of the molecule HXeCl from the reagent $\text{Xe} \cdot \cdot \text{HCl}$ can be described by potential surfaces generated from a more minimal basis set, including the 12 states corresponding to the species N, one state corresponding to I1, and one pertinent to I2. The potential surfaces so obtained are at least semi-quantitatively adequate for describing the processes, although increasing the basis set used in the DIM–DIIS calculation affects the results quantitatively.

II.b. DIM–DIIS Model for Xe_nHCl

The prescription of subsection II.a above provides model electronic states and potential energies for the species $[\text{H} + \text{Xe} + \text{Cl}]$ over the entire range of configurations, so the process $\text{Xe} \cdot \cdot \text{HCl} \rightarrow \text{HXeCl}$ can now be described. This treatment can now be extended to the process in a cluster or matrix environment. The model is constructed from the three species:

$$\begin{aligned}
 \text{A} &\equiv \text{Xe}_{n-1}/\{\text{Xe} + [\text{H}(1\text{S}) + \text{Cl}(^2\text{P})]\} \\
 \text{B} &\equiv \text{Xe}_{n-1}/\{[\text{H}^-\text{Xe}^+(\text{P})] + \text{Cl}(^2\text{P})\} \\
 \text{C} &\equiv \text{Xe}_{n-1}/\{\text{H}(1\text{S}) + [\text{Xe}^+(\text{P})\text{Cl}^-]\}
 \end{aligned} \tag{4}$$

The Xe/Cl^- and Xe/H^- are isotropic atom–ion pair interactions. The $\text{Xe}/\text{Cl}(\text{P})$ interaction is anisotropic, of the DIM type of eqn. (1), and is available. The $\text{Xe}/\text{Xe}^+(\text{P})$ interaction is also anisotropic and can be modeled by DIM, similarly to eqn. (1). So far, we used an isotropic potential approximation for this interaction, and the DIM treatment for this will be introduced as an improvement in the future. The interactions Xe/Xe between neutral atoms are described by available atom–atom pair potentials. Our model differs from the standard DIIS³² in including the ionic form B, in incorporating spin–orbit interactions that are very important here, and in several other details, but qualitatively the approach is very similar.

II.c. “Surface-hopping” MD simulation using the DIM–DIIS potentials

Diagonalization of the DIM–DIIS Hamiltonian for a given nuclear configuration gives the values of the adiabatic PESs, within the model, for that configuration. A calculation using N basic states yields, in principle, N adiabatic PESs. The non-adiabatic coupling between different PESs can also

be computed from the model. The coupling between two adiabatic states, m and n is described by the quantities:

$$C_{mn}^{(\alpha)}(\mathbf{R}) = \left\langle \Phi_m(\gamma, \mathbf{R}) \left| \frac{\partial \Phi_n(\gamma, \mathbf{R})}{\partial R_\alpha} \right\rangle_\gamma \quad (5)$$

Here $\Phi_m(\gamma, \mathbf{R})$, $\Phi_n(\gamma, \mathbf{R})$ are the electronic wavefunctions for the m and n adiabatic states, γ denotes the electronic degrees of freedom, and \mathbf{R} is the nuclear configuration of the system, and R_α is a nuclear coordinate. A more convenient form for the evaluation of $C_{mn}^{(\alpha)}(\mathbf{R})$ in the framework of DIM, based on applying the Hellman–Feynman Theorem to eqn. (5) is:

$$C_{mn}^{(\alpha)}(\mathbf{R}) = \frac{\langle \Phi_m(\gamma, \mathbf{R}) | [\partial H(\gamma, \mathbf{R}) / \partial R_\alpha] | \Phi_n(\gamma, \mathbf{R}) \rangle_\gamma}{W_n(\mathbf{R}) - W_m(\mathbf{R})} \quad (6)$$

where $H(\gamma, \mathbf{R})$ is the electronic Hamiltonian, and $W_m(\mathbf{R})$, $W_n(\mathbf{R})$ are the m and the n adiabatic potential surfaces, all evaluated at nuclear configuration \mathbf{R} . Using the model Hamiltonian of DIM–DIIS, expression (6) can be conveniently computed. For the basis size used here, the calculations of the adiabatic PESs $W_m(\mathbf{R})$, and of the non-adiabatic couplings $C_{mn}^{(\alpha)}$ are efficient to the point that they can be generated and used “on the fly” in the course of dynamics simulations.

To pursue the dynamics of the non-adiabatic processes, we follow the semiclassical “surface hopping” approach of Tully,³⁵ that we previously used also in the studies of photodissociation and recombination of HCl in rare-gas solids and clusters.^{12,16} In this approach, the nuclei are propagated classically on a PES so long as non-adiabatic transitions to other potential surfaces do not take place. Electronic motions are described quantum mechanically by a time-dependent electronic wavepacket, that is a linear combination of the adiabatic electronic eigenstates:

$$\Psi(\gamma, \mathbf{R}, t) = \sum_n C_n(t) \Phi_n(\gamma, \mathbf{R}) \quad (7)$$

The equations of motion for the coefficients $C_n(t)$ include the non-adiabatic couplings, eqn. (6), as well as the adiabatic potentials $W(\mathbf{R})$, and are solved simultaneously with the propagation of the nuclear trajectories $\mathbf{R}(t)$.^{12,35} The “surface hopping” method provides criteria, based on changes in the magnitudes of the $|C_n(t)|$, for the occurrence of non-adiabatic transitions. Such events are modeled by “hopping” of the nuclei from one potential surface $W_n(\mathbf{R})$, to another, $W_m(\mathbf{R})$. The nuclear configuration $\mathbf{R}(t')$ at the instant of the “hopping” t' , is preserved. The procedure continues with propagation of the nuclei on the “new” surface $W_m(\mathbf{R})$, till the electronic equations of motion predict another “hopping” event. The numerical implementation of this scheme, with “on the fly” computation of the DIM–DIIS potential surfaces and non-adiabatic couplings along the trajectories of the nuclear motions, is similar to that for the previous DIM simulations of HCl photodissociation/recombination in rare-gas solids and clusters.^{12,16,28} The numerical effort for the DIM–DIIS model is greater than for the neutral-channel DIM, but for the smallest basis-set sizes we employed it is of the same order of magnitude. So far, only “sample” trajectories were computed, which permit some qualitative insight but are insufficient, *e.g.* for calculations of yields of HXeCl formation. The simulations are being carried out for HCl embedded inside a $(\text{Xe})_{54}$ cluster.

III. Results and discussion

III.a. DIM–DIIS description of HXeCl

A key question of this study is whether the DIM–DIIS model proposed here describes the existence of stable HXeCl, with correct properties. Further on we shall examine whether the model can describe the formation path of the species, from reagent to product.

Fig. 1 shows, qualitatively, the orbitals involved in the DIM–DIIS modeling of HXeCl and of the “reagent” for this species, the cluster $\text{Xe} \cdots \text{HCl}$.

Fig. 2 shows the collinear equilibrium structures predicted by the model for the ionic product species, and also gives the transition state according to DIM–DIIS, which is bent, and corresponds essentially to the configuration at which charge redistribution within the triatomic system takes place on the path from reagent to product.

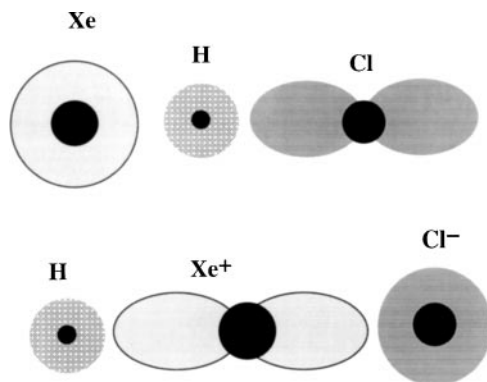


Fig. 1 Orbitals of effective electrons in DIM-DIIS model. Upper part: Σ state of $\text{Xe} \cdots \text{HCl}$ cluster. Lower part: Σ state of HXeCl molecule.

Fig. 3 shows the orbitals in the DIM-DIIS description for a Π state of the reagent and a product. The $^1\Pi_1$ state of the reagents represents the state of the system after photoexcitation, and is essentially a strongly repulsive state.

Fig. 4 shows the potential energy contours around the equilibrium structure of HXeCl . The contours are with respect to the H-Xe and Cl-Xe stretching vibrations of the collinear molecule. These results are very encouraging for the DIM-DIIS model. A stable HXeCl with (nearly) correct interatomic distance is predicted. The harmonic DIM-DIIS H-Xe stretching frequency is 1080 cm^{-1} , the Cl-Xe stretching frequency is around 201 cm^{-1} , both differ substantially from the corresponding values obtained by *ab initio* calculations (1750 and 263 cm^{-1} , respectively), but the level of agreement is adequate for the semiquantitative description required for our purpose. The fact that the potential contours are only moderately anharmonic (also in accord with the *ab initio* results) indicates the stability of the species, at least with regard to the stretching vibrations. The most anharmonic motion in this system is the bending vibration, which if taken to very large displacements will lead to the vicinity of the transition state (and to highly exothermic production

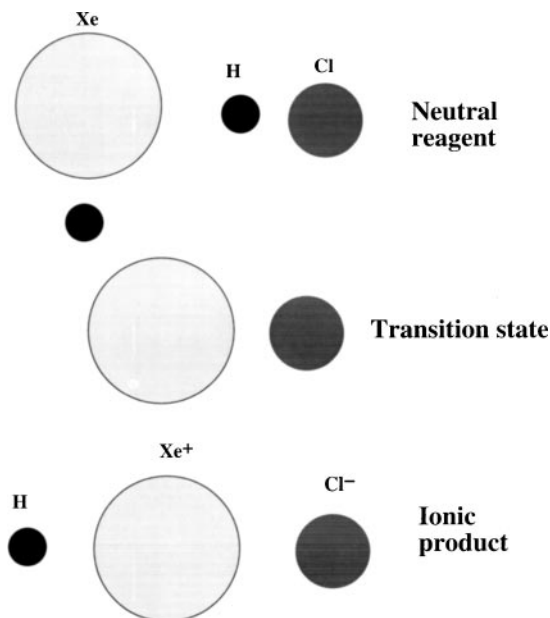


Fig. 2 Geometries of $\text{Xe} \cdots \text{HCl}$ cluster (upper part); HXeCl molecule (lower part); transition state (middle part).

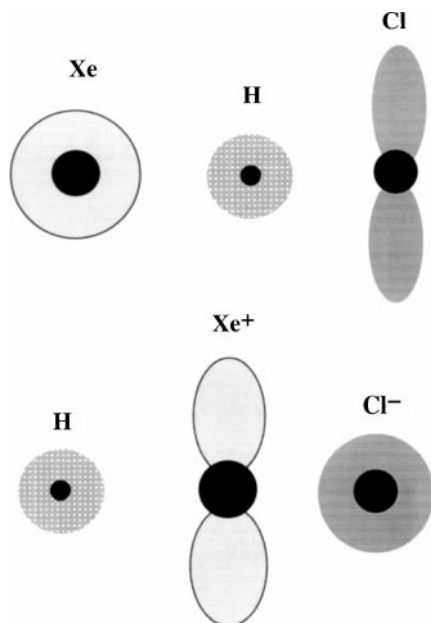


Fig. 3 Orbitals of effective electrons in DIM-DIIS model. Upper part: $^1\Pi$ state of $\text{Xe}\cdots\text{HCl}$ cluster (photoexcited state). Lower part: Π state of HXeCl molecule.

of Xe-HCl). However, this vibration is also stable when not highly excited, with a harmonic frequency of 340 cm^{-1} (the *ab initio* result is 577 cm^{-1}).

Fig. 5 shows the potential energy contours, at collinear configurations, of $\text{Xe} + \text{HCl}$ after photochemical excitation into the $^1\Pi_1$ state. The contours show the highly repulsive nature of this (“reagent”) state. There are no *ab initio* results to compare with, but the results are similar to those seen for empirical potentials on closely related systems such as $\text{Ar} + \text{HCl}$.³⁶

III.b. Potential along the path from $\text{Xe} + \text{HCl}$ to HXeCl

Fig. 6 shows the lowest DIM-DIIS PES along a path leading from the “reagent” zone corresponding to $\text{Xe} + \text{HCl}$ to the HXeCl “product”, in a calculation for the triatomic system

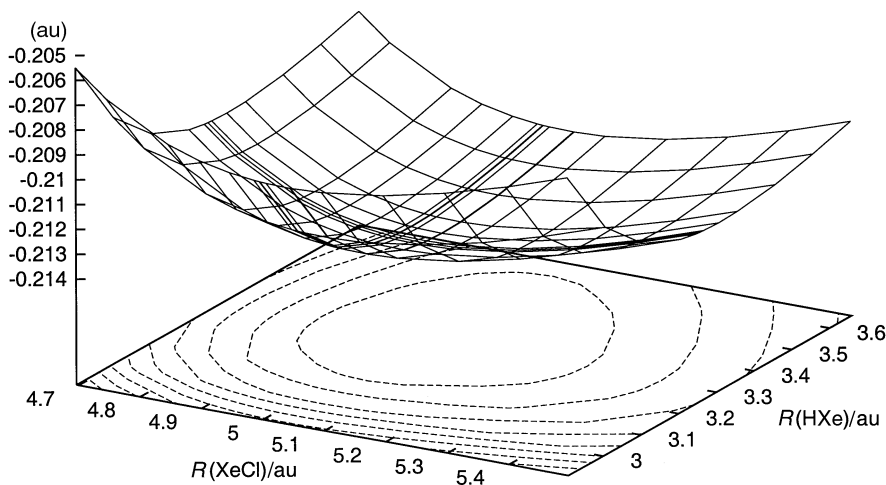


Fig. 4 PES near equilibrium configuration of HXeCl .

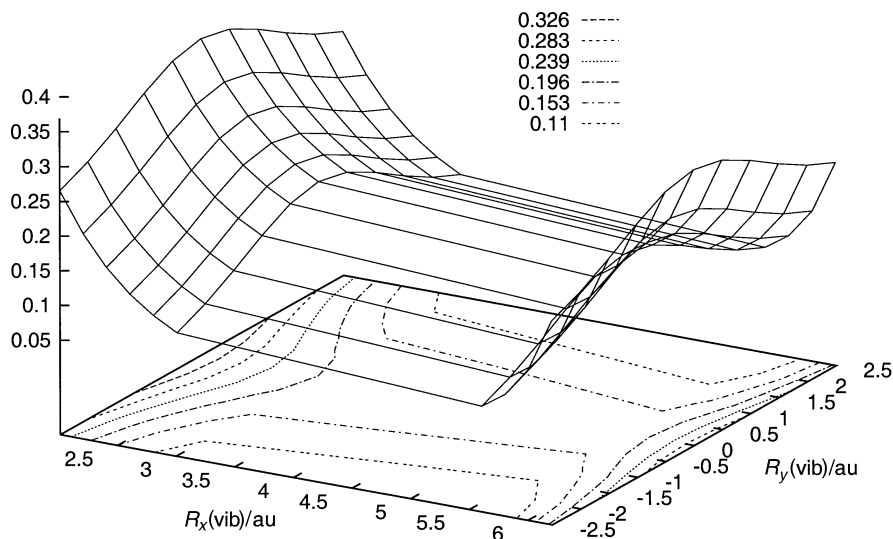


Fig. 5 PES of photoexcited Xe \cdots HCl (reagent zone). The coordinate x is the H position along the Xe \cdots Cl axis, y is the H position normal to this axis.

H + Xe + Cl. The calculation is not strictly for the minimum energy path, but along the bending mode, starting from the equilibrium configuration of HXeCl, and proceeding to increasing bending amplitude. This path corresponds to that adopted by Johansson *et al.*³⁰ in their *ab initio* calculations. As Fig. 6 shows, there is a barrier, which provides chemical stability for HXeCl once formed. The decomposition into Xe + HCl is, of course, highly exothermic. The lifetime of HXeCl in its vibrational ground state due to tunneling through the barrier is, according to estimates exceedingly long, to the point that the species can be considered completely stable at $T = 0$ K. This, of course, is in accord with the experimental data.¹⁹ Obviously, tunneling is likewise far too slow to play a role in the reverse process, HXeCl formation. Comparison of Fig. 6 with the *ab initio* results of Johansson *et al.* is encouraging for DIM-DIIS. The DIM-DIIS barrier along the bending mode has its maximum at 110° . (The *ab initio* result is $\sim 105^\circ$), and the barrier height against the isomerization of HXeCl into Xe + HCl is 0.26 eV (the *ab initio* value is 1.4 eV). As

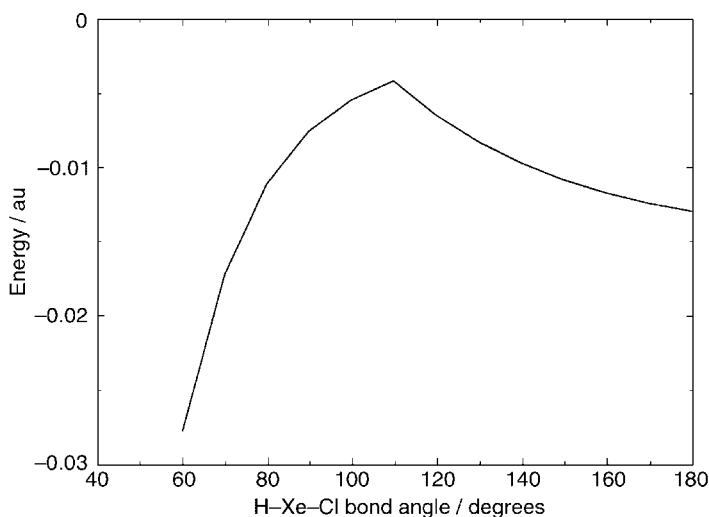


Fig. 6 The lowest PES of HXeCl along the bending mode.

this, and as the results of the previous subsection show, the DIM–DIIS are semiquantitatively adequate. The model predicts the correct type of interactions, the correct geometries of species and the correct barrier positions, with barrier heights, frequencies, *etc.* of the right order of magnitude. DIM–DIIS is thus suitable as a model for the formation mechanisms of HXeCl, but quantitative modeling requires much more accurate potential surfaces.

III.c. Role of non-adiabatic transitions in HXeCl formation in the cluster

While in the previous subsections the focus was on the lowest adiabatic PES that leads from the reagents to the HXeCl species, non-adiabatic transitions do in fact play a major role in the formation dynamics of HXeCl in the cluster (or matrix). This conclusion follows from analogues of the DIM–DIIS PESs and non-adiabatic couplings, from several sample trajectories of the “surface hopping” trajectories, and from previous extensive “surface hopping” simulations of the related system of HCl in argon clusters and solids.^{12,16} There are at least two types of non-adiabatic transitions that are important here. First, consider the photoexcitation state. The $^1\Pi$ state of $H + Cl(^2P)$ is initially populated at the reagent configurations. This state is repulsive, but cage exit of the energetic H atom produced is not necessarily direct. In most trajectories, the H atom recoils from the cage walls upon the first collision. Non-adiabatic transitions from the nascent $^1\Pi$ state can take place. The yield for such transitions seems substantial and the results affect the subsequent dynamics, including HXeCl formation. Indeed, for the related system of $Ar_{54}(HCl)$, for which extensive trajectory statistics are available,¹⁶ about 7% of the excited molecules reach the $^1\Sigma_0$ electronic state, and $H + Cl$ recombination takes place. This obviously limits the fraction of $H + Cl$ that can form HXeCl. Much larger than the number of recombination events, is the number of cases where the $H + Cl(^2P)$ makes a transition into a repulsive PES other than that corresponding to the $^1\Pi$ initially excited state. Recombination is only possible on the one attractive state of the system, $^1\Sigma_0$. However, H atoms that exit the cage after non-adiabatic transitions into states other than $^1\Pi$, tend to have at least somewhat reduced kinetic energies upon exit. This effect reduces the yield for HXeCl formation. We conclude that non-adiabatic transitions in the reagent cage play an important role in influencing the formation probabilities.

A second type of non-adiabatic transitions seem to occur for configurations that correspond approximately to the barrier for HXeCl formation, in Fig. 6. Such configurations can be realized in the cluster only for H atoms that exited the reagent cage. The position of the barrier in Fig. 6 corresponds to configurations for which charge transfer takes place in the $H + Xe + Cl$ system, and the ionic species HXeCl is formed. There are near-crossings between the lowest PES and higher PESs in this region, the DIM–DIIS non-adiabatic couplings are large for these configurations, and the probabilities for non-adiabatic transitions are thus substantial. In summary, there are appreciable non-adiabatic events in the region of transition between the “neutral” and “ionic” species of the DIM–DIIS model.

There are a number of ionic PESs produced by DIM–DIIS at the configurations of HXeCl. We did not yet explore the issue of non-adiabatic transitions between these surfaces, *i.e.* after HXeCl is formed. Tentatively, the impression is that after an ionic species HXeCl is formed in the cluster (or matrix), electronic (as well as vibrational) relaxation that stabilizes the product is very fast, so such non-adiabatic transitions are not important for the formation dynamics.

III.d. Formation dynamics of HXeCl in the cluster

Fig. 7 shows snapshots of a trajectory of HXeCl formation, that we suppose to be typical.

As discussed in the previous subsections, geometric considerations suggest that H exit from the reagent cage is a precondition for HXeCl formation. After the exit, the H atom in the snapshots has collided with a Xe atom farther away from the cage, and has recoiled towards a Xe atom of the original reagent cage. That Xe atom is now between the Cl atom and the H atom. The triatomic system is at a configuration close to the transition state of Fig. 6. Charge transfer takes place, and the ionic species $H^{(-\alpha)}Xe^{(+\beta)}Cl^{(-\gamma)}$ is formed. Thus, the kinetic energy of the H atom serves to excite the stable closed-shell structure of the Xe, and the product formed was stabilized by the partly ionic H–Xe and Xe–Cl bonds thus formed. The HXeCl was formed in this case in its ground electronic state (lowest-lying ionic state of the system), but initially has a considerable amount of vibrational energy. The coupling between the ionic species and the cluster environment is relatively strong (considerably more so than for neutral species in the rare-gas medium), and

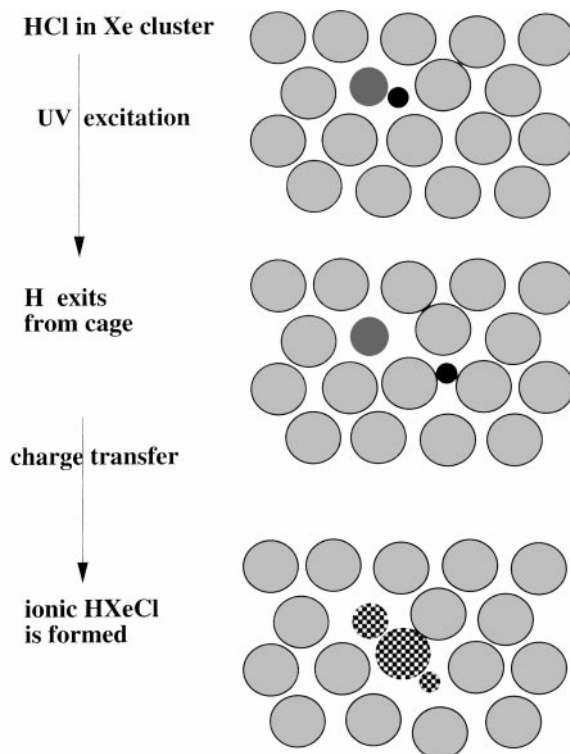


Fig. 7 Snapshots showing stages in formation of HXeCl following photolysis of HCl in Xe clusters.

vibrational energy relaxation of the HXeCl is thus quite fast (a timescale of picoseconds is estimated). Once vibrationally relaxed, the HXeCl species is stable, though the cluster is hot, and evaporation of Xe atoms (not shown) begins to take place.

IV. Concluding remarks

A variant of the DIM–DIIS model was developed and applied to the PESs describing the formation of the molecule HXeCl, following photolysis of HCl in xenon clusters. The model was found adequate, at least semiquantitatively, in describing the system. It correctly predicts the structure of the species involved (product as well as reagents), the nature of the interactions, the barrier position and heights, and the frequencies. The merit of the model is that it yields global, easy to compute potential surfaces for the system, including the cluster atoms. This makes MD simulations possible, and the formation of HXeCl can be investigated both from the properties of the potential surfaces, and of the dynamics in time. In an essentially qualitative study, the mechanism of formation was clarified. It requires exit of the photoproduced H atom from the reagent cage. When this H atom hits the second ‘wall’ of Xe, it may recoil towards a xenon atom of the cage, the H atom and the Cl atom can therefore simultaneously collide with the same xenon atom hitting it on opposite ends. Rapid charge transfer takes place, and the species HXeCl, with a strongly ionic character is formed. Non-adiabatic processes were found important in the process, which is the reason why “surface hopping” (or similar) simulations of the formation dynamics are essential. The non-adiabatic processes that play a role are those in the reagent region (which corresponds to non-radiative electronic relaxation of the photoexcited HCl), and also those that take place at configurations corresponding to the transition between the neutral and ionic $\text{H} + \text{Xe} + \text{Cl}$ species. It is suggested that the ionic character of the HXeCl formed plays an important role in the stabilization of the species, because of the strong coupling to the cluster vibrations, which removes vibrational energy from the nascent HXeCl.

An advantage of the DIM–DIIS approach proposed here is that it can be easily applied to any of the new HRgX molecules. It may not only help interpret experimental data for existing systems, but perhaps may also predict novel, yet unknown, systems of this family.

On the other hand, the level of the potential surfaces is such that they can probably not be trusted for quantitative predictions (*e.g.* of formation yields, which are of great interest). This requires the development of much better potentials that can yield more reliable barrier heights. Such a goal is in our view quite attainable.

Acknowledgements

We thank Dr. Nicholas Wright, Dr. Galiana Chaban and Dr. J. Lundell for many helpful discussions and suggestions. We are also grateful to Dr. I. Last for useful remarks.

This research was supported by the DFG (Germany), in the framework of the project Sfb 450, “Analysis and Control of Ultrafast Reactions”. The research was also supported in part by a grant from the Israel Science Foundation (to RBG).

References

- 1 N. Bartlett, *Proc. Chem. Soc.*, 1962, 218.
- 2 J. J. Turner and G. C. Pimental, *Science*, 1963, **140**, 974.
- 3 L. Stein, *Nature*, 1973, **243**, 30.
- 4 J. H. Holloway and E. G. Hope, *Adv. Inorg. Chem.*, 1999, **46**, 51.
- 5 V. A. Apkarian and N. Schwentner, *Chem. Rev.*, 1999, **99**, 1401.
- 6 V. E. Bondybey and L. E. Brus, *J. Chem. Phys.*, 1975, **62**, 620.
- 7 M. E. Fajardo and V. A. Apkarian, *J. Chem. Phys.*, 1986, **85**, 5660.
- 8 R. Zadoyan, J. Almy and V. A. Apkarian, *Faraday Discuss.*, 1997, **108**, 255.
- 9 J. G. McCaffrey, H. Kunz and N. Schwentner, *J. Chem. Phys.*, 1992, **96**, 155.
- 10 V. Batista and D. Coker, *J. Chem. Phys.*, 1997, **106**, 6923.
- 11 R. Alimi, R. B. Gerber and V. A. Apkarian, *J. Chem. Phys.*, 1988, **89**, 174.
- 12 A. I. Krylov and R. B. Gerber, *J. Chem. Phys.*, 1997, **106**, 6574.
- 13 R. B. Gerber, A. B. McCoy and A. Garcia-Vela, *Annu. Rev. Phys. Chem.*, 1994, **45**, 275.
- 14 J. Segall, Y. Wen, R. Singer, C. Wittig, A. Garcia-Vela and R. B. Gerber, *Chem. Phys. Lett.*, 1993, **207**, 504.
- 15 Q. Lin, J.-L. Wang and A. H. Zewail, *Nature*, 1993, **364**, 427.
- 16 M. Y. Niv, A. I. Krylov and R. B. Gerber, *Faraday Discuss.*, 1997, **108**, 243.
- 17 (a) M. Pettersson, J. Lundell and M. Räsänen, *J. Chem. Phys.*, 1995, **102**, 6423; (b) M. Pettersson, J. Nieminen, L. Khriachtchev and M. Räsänen, *J. Chem. Phys.*, 1997, **107**, 8423.
- 18 M. Pettersson, L. Khriachtchev, J. Lundell and M. Räsänen, *J. Am. Chem. Soc.*, 1999, **121**, 11904.
- 19 M. Pettersson, J. Lundell and M. Räsänen, *Eur. J. Inorg. Chem.*, 1999, 729.
- 20 M. Pettersson, L. Khriachtchev, J. Lundell, S. Jolkkonen and M. Räsänen, *J. Phys. Chem. A*, 2000, **104**, 3579.
- 21 L. Khriachtchev, M. Pettersson, N. Runeberg, J. Lundell and M. Räsänen, *Nature*, 2000, **406**, 874.
- 22 J. Lundell, M. Pettersson, L. Khriachtchev, M. Räsänen, G. M. Chaban and R. B. Gerber, *Chem. Phys. Lett.*, 2000, **322**, 389.
- 23 J. Lundell, G. M. Chaban and R. B. Gerber, *J. Phys. Chem. A*, 2000, **104**, 7944.
- 24 J. Lundell, G. M. Chaban and R. B. Gerber, *Chem. Phys. Lett.*, 2000, **331**, 308.
- 25 F. O. Ellison, *J. Am. Chem. Soc.*, 1963, **85**, 3540.
- 26 P. J. Kunz, in *Atom–Molecules Collision Theory—A Guide for the Experimentalist*, ed. R. B. Bernstein, Plenum Press, New York, 1979.
- 27 A. A. Bruchachenko and N. F. Stepanov, *J. Chem. Phys.*, 1997, **106**, 4358.
- 28 M. Y. Niv, A. I. Krylov, R. B. Gerber and U. Buck, *J. Chem. Phys.*, 1999, **110**, 11047.
- 29 R. Baumfalk, N. H. Nahler, U. Buck, M. Y. Niv and R. B. Gerber, *J. Chem. Phys.*, 2000, **113**, 329.
- 30 M. Johansson, M. Motokka, M. Pettersson and M. Räsänen, *Chem. Phys.*, 1999, **244**, 25.
- 31 I. Last and T. F. George, *J. Chem. Phys.*, 1987, **87**, 1183.
- 32 I. Last and T. F. George, *J. Chem. Phys.*, 1988, **89**, 3071.
- 33 M. Bettendorff, S. D. Peyerimhoff and R. J. Buenker, *Chem. Phys.*, 1982, **66**, 261.
- 34 G. A. Gallup and J. Macek, *J. Phys. B*, 1977, **10**, 1601.
- 35 J. C. Tully, *J. Chem. Phys.*, 1990, **93**, 1061.
- 36 A. Garcia-Vela, R. B. Gerber and D. G. Imre, *J. Chem. Phys.*, 1992, **97**, 7242.